Environmental Science & Technology

pubs.acs.org/est

Article

# Tracking Air Pollution in China: Near Real-Time $PM_{2.5}$ Retrievals from Multisource Data Fusion

Guannan Geng, Qingyang Xiao, Shigan Liu, Xiaodong Liu, Jing Cheng, Yixuan Zheng, Tao Xue, Dan Tong, Bo Zheng, Yiran Peng, Xiaomeng Huang, Kebin He, and Qiang Zhang*

Cite This: https://doi.org/10.1021/acs.est.1c01863

Read Online

ACCESS | Metrics & More | Article Recommendations | Supporting Information

**ABSTRACT:** Air pollution has altered the Earth's radiation balance, disturbed the ecosystem, and increased human morbidity and mortality. Accordingly, a full-coverage high-resolution air pollutant data set with timely updates and historical long-term records is essential to support both research and environmental management. Here, for the first time, we develop a near real-time air pollutant database known as Tracking Air Pollution in China (TAP, http://tapdata.org.cn/) that combines information from multiple data sources, including ground observations, satellite aerosol optical depth (AOD), operational chemical transport model simulations, and other ancillary data such as meteorological fields, land use data, population, and elevation. Daily full-coverage $PM_{2.5}$ data at a spatial resolution of 10 km is our first near real-time product. The TAP $PM_{2.5}$ is estimated based on a two-stage machine learning model coupled with the synthetic minority oversampling technique and a tree-based gap-filling method. Our model has an averaged out-of-bag cross-validation $R^2$ of 0.83 for different years, which is comparable to those of other studies, but improves its performance at high pollution levels and fills the gaps in missing AOD on daily scale. The full coverage and near real-time updates of the daily $PM_{2.5}$ data allow us to track the day-to-day variations in $PM_{2.5}$ concentrations over China in a timely manner. The long-term records of $PM_{2.5}$ data since 2000 will also support policy assessments and health impact studies. The TAP $PM_{2.5}$ data are publicly available through our website for sharing with the research and policy communities.

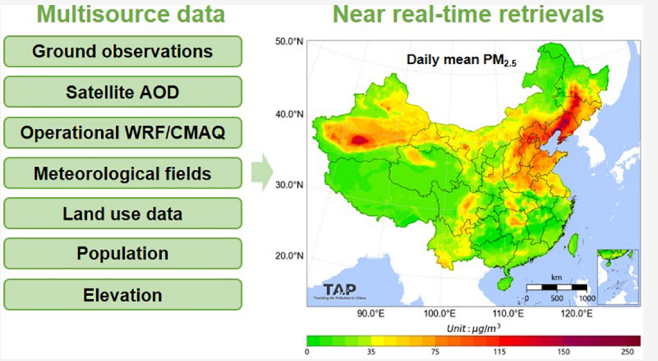


**KEYWORDS:** *$PM_{2.5}$, random forest, air pollution, exposure assessment, satellite remote sensing*



## 1. INTRODUCTION

With rapid urbanization and economic growth, anthropogenic emissions of reactive gases, aerosols, and aerosol precursors are being emitted into the atmosphere, and these substances substantially changed the atmospheric composition. Consequently, worsening air pollution has altered the Earth's radiation balance, distressed the ecosystem and increased the risks of human morbidity and mortality.[1,2] In particular, one of the major air pollutants in China is fine particulate matter ($PM_{2.5}$), which could cause serious health problems[3,4] and reduce visibility.[5] Hence, understanding the spatial and temporal variations of ambient $PM_{2.5}$ concentrations constitutes the basis for research studies associated with air pollution, climate change, and environmental health. It follows, then, that a complete-coverage high-resolution $PM_{2.5}$ data set with timely updates and historical long-term records is essential to support both scientific research and environmental management. A complete-coverage data set would allow us to obtain a full spatial picture of $PM_{2.5}$ pollution and identify heavily polluted areas that cannot be shown by the ground monitoring stations. Full-coverage data set can also help to avoid exposure misclassification in epidemiological studies.[6,7] Moreover, real-time or near real-time updates of $PM_{2.5}$ data would help us track substantial changes in air pollution during haze events or special times such as the coronavirus pandemic. It could also be linked to real-time or near real-time acute effects of air pollution such as asthma flare-ups, hospital admissions and premature deaths, and alert the population for real-time public health prevention. In addition, a historical long-term data set benefiting from a consistent methodology could support clean air policy assessments and chronic health impact studies.[8−11]

Several data sources could provide information about $PM_{2.5}$ pollution. Among them, ground measurements are the most accurate way to obtain ambient $PM_{2.5}$ concentrations.

Received: March 22, 2021
Revised: August 4, 2021
Accepted: August 4, 2021

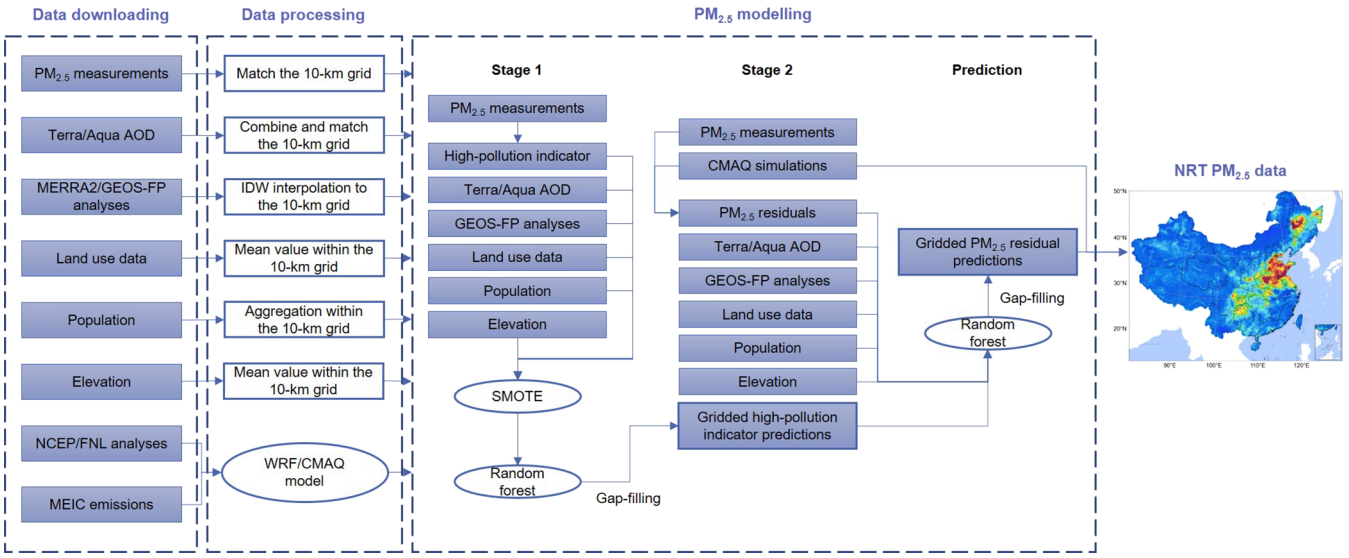


**Figure 1.** Operational process of the near real-time $PM_{2.5}$ data generated from TAP.

**Table 1. Summary of the Datasets Used in This Study from Multiple Sources**

| data category | data name | spatial resolution | temporal frequency | time coverage | data source |
|---|---|---|---|---|---|
| ground observations | $PM_{2.5}$ measurements | point | hourly | 2013 to date | http://www.cnemc.cn/ |
| satellite AOD | MODIS Terra AOD | ~10 km | daily | 2000 to date | https://ladsweb.modaps.eosdis.nasa.gov/ |
| | MODIS Aqua AOD | ~10 km | daily | 2000 to date | https://ladsweb.modaps.eosdis.nasa.gov/ |
| operational WRF/CMAQ | NCEP/FNL | 1° | daily | 2000 to date | https://rda.ucar.edu/datasets/ds083.2/ |
| | NCEP/GFS | 1° | daily | 2000 to date | https://www.nco.ncep.noaa.gov/pmb/products/gfs/ |
| | MEIC emissions | 36 km | monthly | 2000 to date | http://meicmodel.org/ |
| | CMAQ simulations | 36 km | daily | 2000 to date | - |
| meteorological fields | MERRA-2 | 0.5°×0.625° | 3-hly | 2000 to date | https://gmao.gsfc.nasa.gov/reanalysis/MERRA-2/ |
| | GEOS-FP | 0.5°×0.625° | 6-hly | 2011 to date | https://gmao.gsfc.nasa.gov/GMAO_products/NRT_products.php |
| land use data | FROM-GLC | 30 m | yearly | 2000−2018 | http://data.ess.tsinghua.edu.cn/ |
| population | GPW v4 | 1 km | yearly | 2000 to date | https://beta.sedac.ciesin.columbia.edu/ |
| | WorldPop | county | yearly | 2000 to date | https://www.worldpop.org/ |
| | China City Yearbooks | national | yearly | 2000 to date | https://data.cnki.net/ |
| elevation | GDEM | 30 m | - | - | https://earthexplorer.usgs.gov/ |

However, due to the installation and maintenance costs of ground networks, monitoring stations are usually sparse and unevenly distributed, with most of the stations located in urban areas.[11,12] Moreover, $PM_{2.5}$ ground networks in China were established in 2013, so prior data are unavailable. As an alternative, chemical transport models (CTMs) could provide complete-coverage simulations of $PM_{2.5}$ concentrations and could reproduce the spatial and temporal trends of $PM_{2.5}$ concentrations when using reasonable emission inventories.[10,13] However, biases still exist in the simulated absolute values of $PM_{2.5}$ due to uncertainties in emission inventories[14] and the lack of certain physical and chemical processes in the model.[15−17] Satellite-retrieved aerosol optical depth (AOD) data, which can reflect the aerosol abundance in the atmosphere, have the advantage of long-term records and a high resolution. However, AOD data are missing during haze events, on cloudy days, and over bright surfaces such as desert and areas covered with snow, and the spatial distribution of missing data is sometimes nonrandom, which might cause biases in the long term average value.[18] Accordingly, a data set that combines data from multiple sources is needed to take advantage of all available information and to meet the requirements of such a data set, namely, a high accuracy, a full spatial coverage, a long temporal span, and real-time updates.

Previous studies have developed different methods to fuse two or more of the above data sets with other ancillary data in China to improve the estimation of $PM_{2.5}$.[19−28] These methods include CTM-based algorithms,[26,27] physical models,[21] statistical models such as linear mixed-effects models and generalized additive models,[19,22] and machine learning models such as random forest and extreme gradient boosting.[20,23−25,28] As a result, numerous researchers have developed historical data sets in China, for example, 10 km $PM_{2.5}$ data between 2000 and 2016 by Xue et al.[25] and 1 km $PM_{2.5}$ data between 2000 and 2018 by Wei et al.[23] However, only some of these studies fill the gaps in AOD data using CTM simulations on a daily scale and achieve full-coverage daily $PM_{2.5}$ concentrations.[24,25,28] And previous studies usually underestimate $PM_{2.5}$ concentrations on highly polluted days (e.g., $PM_{2.5}$ > 150 $\mu g/m^3$) due to the small sample size of high-pollution cases and highly nonlinear relationship between $PM_{2.5}$ and


https://doi.org/10.1021/acs.est.1c01863
Environ. Sci. Technol. XXXX, XXX, XXX−XXX

AOD.[25,29] Furthermore, none of these works provide near real-time $PM_{2.5}$ data publicly to support real-time public health prevention. Consequently, a near real-time data set with gap-filled daily $PM_{2.5}$ estimates in China that can be shared with the research and policy communities remains lacking.

In this study, we develop the Tracking Air Pollution in China (TAP, http://tapdata.org.cn/) database based on an operational CTM, a two-stage machine learning model and a gap-filling method.[30] Our goal is to combine information from multiple data sources and provide near real-time (i.e., one-day delay) $PM_{2.5}$ data on a daily scale with complete coverage at a spatial resolution of 10 km since 2000 to support related studies and environmental management. TAP is fully integrated on the cloud-computing platform, which allows users to conveniently access all customized data products online. Due to the downloading, processing and modeling procedures, the $PM_{2.5}$ data of the previous day are available to the public at approximately 9:00 AM Beijing time.

## 2. DATA AND METHODS

Figure 1 shows the modeling framework of the TAP $PM_{2.5}$ data set, including input data obtained from multiple data sources, processing of the input data, and the models developed to fuse the multisource data and generate near real-time $PM_{2.5}$ retrievals.

**2.1. Multisource Input Data.** Table 1 summarizes all the input data used in this study, including ground observations, satellite AOD, operational Weather Research and Forecasting/Community Multiscale Air Quality Modeling System (WRF/CMAQ), and other ancillary data such as meteorological fields, land use data, total population, and elevation. The $PM_{2.5}$ measurements updated every hour are collected from the national air quality monitoring network (http://www.cnemc.cn/) in China, which includes ~1600 stations over China. Continuous identical data over 3 h are excluded, and then the daily mean $PM_{2.5}$ is calculated only if at least 12 hourly measurements are available. The $PM_{2.5}$ measurements are matched to the 10 km grid cells they fall in.

Moderate Resolution Imaging Spectroradiometer (MODIS) Collection 6 level 2 aerosol products[31] from both Aqua and Terra at a spatial resolution of 0.1° are downloaded from the National Aeronautics and Space Administration (NASA, https://ladsweb.modaps.eosdis.nasa.gov/) of the United States. We use AOD measurements retrieved by both the Dark Target (DT) algorithm[31] and the Deep Blue (DB) algorithm[32] from Terra and Aqua to improve the spatial coverage of AOD data. A daily linear regression is first fitted between the DT and DB AOD when both are available for Terra and Aqua separately and then used to fill the missing AOD when only the DT AOD or the DB AOD is valid. Then, the AOD averaged between the DT and DB AOD is calculated for Terra and Aqua separately. Similarly, a second linear regression is fitted between the Terra and Aqua AOD to fill the missing AOD when only one of them is available. The average Terra and Aqua AOD is used to represent the daily aerosol loading.[33]

The WRF/CMAQ modeling system is included in our work to provide daily $PM_{2.5}$ simulations. We employ the National Center for Environmental Prediction Final Analysis (NCEP-FNL, https://rda.ucar.edu/datasets/ds083.2/) and the Global Forecast System (NCEP-GFS, https://www.nco.ncep.noaa.gov/pmb/products/gfs/) to drive the WRF model. Anthropogenic emissions are taken from the Multiresolution Emission Inventory in China (MEIC, http://meicmodel.org/),[34,35] which is updated in a timely manner using a bottom-up approach based on near real-time activity indicators.[36] More details about the dynamic emissions can be found in Zheng et al.,[36] and a more in-depth description of the WRF/CMAQ model is provided in Section 2.2.1. Daily $PM_{2.5}$ simulations from the WRF/CMAQ model are interpolated into the 10 km grid using the inverse distance weighting (IDW) method.

The meteorological analysis data are taken from the Modern-Era Retrospective Analysis for Research and Applications Version 2 (MERRA-2) data set at a resolution of 0.5° × 0.625°[37] and the Goddard Earth Observing System Forward Processing (GEOS-FP) data set at a resolution of 0.25° × 0.3125°.[38] We utilize the following parameters extracted from the analysis data: surface albedo, surface pressure, surface incoming shortwave flux, surface net downward shortwave flux, surface net downward longwave flux, total incoming shortwave flux, total net downward shortwave flux, total latent energy flux, cloud area fraction for low clouds, total cloud area fraction, total column ozone, total column odd oxygen, bias-corrected total precipitation, total precipitable ice water, total precipitable water vapor, total precipitable liquid water, evaporation from turbulence, 2 m specific humidity, 2 m dew point temperature, 2 m air temperature, 2 m eastward wind (U wind), 2 m northward wind (V wind), 10 m U wind, 10 m V wind, 10 m wind speed, U wind at 500 hPa, V wind at 500 hPa, U wind at 850 hPa, V wind at 850 hPa, planetary boundary layer height, and snowfall. Daily averaged meteorological analysis data are interpolated into the 10 km grid using the IDW approach.

We also download the urban and rural land cover classification data at a spatial resolution of 30 m from Gong et al.[39] (http://data.ess.tsinghua.edu.cn/) and elevation data at a spatial resolution of 30 m from the Global Digital Elevation Model (GDEM) version 2 (https://earthexplorer.usgs.gov/). Population data at a spatial resolution of 1 km are taken from the Gridded Population of the World (GPW) version 4 data set and are calibrated using the WorldPop data set at the county level and the total population reported in China City Yearbooks. The land cover data and elevation data are averaged within the 10-km grid while the population data are summed within the 10-km grid.

**2.2. Algorithm Description.** *2.2.1. Operational WRF/CMAQ Modeling System.* The TAP database includes an operational WRF/CMAQ modeling system to provide daily $PM_{2.5}$ simulations as one of the input data sources, which could improve the accuracy of $PM_{2.5}$ estimations and fill the gaps caused by missing AOD data. The WRF model version 3.9.1 and CMAQ model version 5.2 (https://www.cmascenter.org/cmaq/) are used in our work. The simulation domain covers all of China with a horizontal resolution of 36 km. The vertical resolution is designed as 46 sigma levels from the ground surface to 100 hPa for WRF but only 28 vertical layers in CMAQ after the processing of the Meteorology-Chemistry Interface Processor. For the WRF model, the NCEP-FNL and NCEP-GFS data are used to provide the initial and boundary conditions, whereas the NCEP-GFS sea surface temperature reanalysis data and NCEP Automated Data Processing global observational weather data are used for analysis, observation, and soil nudging. The parametrization scheme follows Cheng et al.[40] with the Kain-Fritsch cumulus physics scheme version 2[41] modified to the Grell-Freitas ensemble scheme.[42] For the CMAQ model, we use the CB05 gas-phase mechanism with


https://doi.org/10.1021/acs.est.1c01863
Environ. Sci. Technol. XXXX, XXX, XXX−XXX

Table 2. Model Performance Compared with Other Studies Developing National $PM_{2.5}$ Datasets in China

| | gap-filled | spatial resolution | temporal resolution | CV type | CV $R^2$ | RMSE ($\mu g/m^3$) |
|---|---|---|---|---|---|---|
| Ma et al.[22] | no | 10 km | daily (2004−2013) | 10-fold CV | 0.79 | 27.4 |
| Fang et al.[19] | no | 10 km | daily (2013−2014) | 10-fold CV | 0.80 | 22.8 |
| He and Huang[53] | no | 3 km | daily (2015) | 10-fold CV | 0.80 | 18.0 |
| Xiao et al.[24] | yes | 10 km | daily (2013−2017) | 10-fold CV | 0.79 | 21.0 |
| Xue et al.[25] | yes | 10 km | daily (2000−2016) | by-year CV | 0.61 | 27.8 |
| Liang et al.[20] | yes | 1 km | monthly (2000−2016) | 10-fold CV | 0.93 | 6.2 |
| Wei et al.[23] | no | 1 km | daily (2013−2018) monthly (2000−2018) | 10-fold CV | 0.86−0.90 | 10.0−18.4 |
| Huang et al.[28] | yes | 1 km | daily (2013−2019) | 10-fold CV | 0.87−0.88 | 11.9−21.9 |
| | | | | by-year CV | 0.62 | 27.7 |
| TAP $PM_{2.5}$ | yes | 10 km | daily (2000−current) | out-of-bag CV (individual years) | 0.80−0.88 | 13.9−22.1 |
| | | | | spatial CV (individual years) | 0.69−0.83 | 14.6−26.4 |
| | | | | by-year CV (hindcast model) | 0.58 | 27.5 |

the CMAQv5.1 update and sixth-generation CMAQ aerosol mechanism (AERO6).

The dynamically updated anthropogenic emissions for mainland China are taken from the MEIC.[34−36] Emissions for other Asian countries and regions are obtained from the MIX inventory.[43] Biogenic emissions are calculated by the Model of Emissions of Gases and Aerosols from Nature (MEGAN) version 2.1.[44] Sea salt and dust aerosol emissions are calculated online by the CMAQ model.

The simulated $PM_{2.5}$ concentrations from our WRF/CMAQ model have been fully evaluated against ground measurements in our previous studies.[10,40,45] Accordingly, the model performance statistics can meet the recommended performance criteria, and the simulated results have been used for policy assessment and health impact studies in China.[10,40,45]

*2.2.2. Two-Stage Machine Learning Model.* A two-stage machine learning model coupled with the synthetic minority oversampling technique (SMOTE) developed in our previous study[46] is used to generate the TAP $PM_{2.5}$ data, as presented in Figure 1. In the first stage, we define a high-pollution indicator to improve the $PM_{2.5}$ estimations on highly polluted days, when $PM_{2.5}$ are usually underestimated in statistical and machine learning models.[23,28] This high-pollution indicator is calculated based on $PM_{2.5}$ observation data and describes whether the $PM_{2.5}$ observations at each location exceed the monthly mean by two standard deviations. As high-pollution events cover only 3.9% of our training data set, which hinders the model's ability to characterize the associations between high-pollution events and other predictors, we adopt the SMOTE technique to resample our data set and obtain a balance between high-pollution and normal samples. The resampled data set is then used to train the first-stage random forest model with all the input data except for the CMAQ simulations, after which the predicted full-coverage high-pollution indicator is passed to the second-stage model as one of the input data. In the second stage, we use the residuals between the $PM_{2.5}$ measurements and the CMAQ $PM_{2.5}$ simulations as the dependent variable to train the second-stage random forest model. The predicted residuals combined with the CMAQ simulations represent the final $PM_{2.5}$ estimations.

Compared with the models presented in previous studies, our model has two major advantages. In the first stage, the SMOTE algorithm balances the uneven proportion of high-pollution and normal data, which could improve the model performance at high $PM_{2.5}$ levels. In the second stage, using the residuals between simulated and measured $PM_{2.5}$ enhances the variability of the dependent data, which could enhance the responses of predictors to $PM_{2.5}$ variations, thus improving the prediction accuracy. We design a sensitivity test model (Sens) without the SMOTE technique and using $PM_{2.5}$ measurements as the dependent variable to show our model improvements.

*2.2.3. Gap-Filling Method.* Our previous study[30] evaluated different gap-filling strategies and proposed a binary tree-based algorithm coupled with WRF/CMAQ simulations to fill the gaps in missing AOD. As the missingness of satellite AOD are primarily related to meteorological conditions (e.g., cloudy, rainy days) and $PM_{2.5}$ pollution (e.g., highly polluted days), the tree-based algorithm could directly predict missing $PM_{2.5}$ by mining the relationship between availability status of satellite data, $PM_{2.5}$ concentrations and other Supporting Information.[47] This method is robust at characterizing the spatial patterns of $PM_{2.5}$ without generating artificially oversmoothed $PM_{2.5}$ spatial distributions and is efficient for use in a near real-time data product.[30] In each step of our two-stage model, a dichotomous predictor defined by whether the satellite AOD is available is constructed as the cut point of the first layer of the decision tree. This predictor serves to build the associations between satellite AOD availability, $PM_{2.5}$ concentration, and other supportive information, such as WRF/CMAQ simulations and meteorological conditions, and helps to fill the gaps in the final $PM_{2.5}$ estimations.

**2.3. Operational Process of the TAP $PM_{2.5}$ Data.** Figure 1 shows the operational process for generating the near real-time $PM_{2.5}$ product in TAP, which includes three steps: data downloading, data processing and $PM_{2.5}$ modeling. Data from multiple sources (summarized in Table 1) are routinely downloaded to the cloud-computing platform every day once they are available. As these data are at different temporal and spatial resolutions, they are processed to match the 10 km grid defined in our work, as described in Section 2.1. Typically, the downloading and processing of the multisource input data are finished around 5:10−6:20 AM Beijing time.

Models are trained using input data from different time periods to develop $PM_{2.5}$ data from 2000 to date. For years when ground $PM_{2.5}$ measurements are available (i.e., 2013−2020), individual models are developed for these years using input data within each year. For the hindcast of $PM_{2.5}$ prior to 2013 when ground measurements are absent, a model trained with data set between 2013−2019 is developed and validated to provide robust hindcasting power.


https://doi.org/10.1021/acs.est.1c01863
Environ. Sci. Technol. XXXX, XXX, XXX−XXX

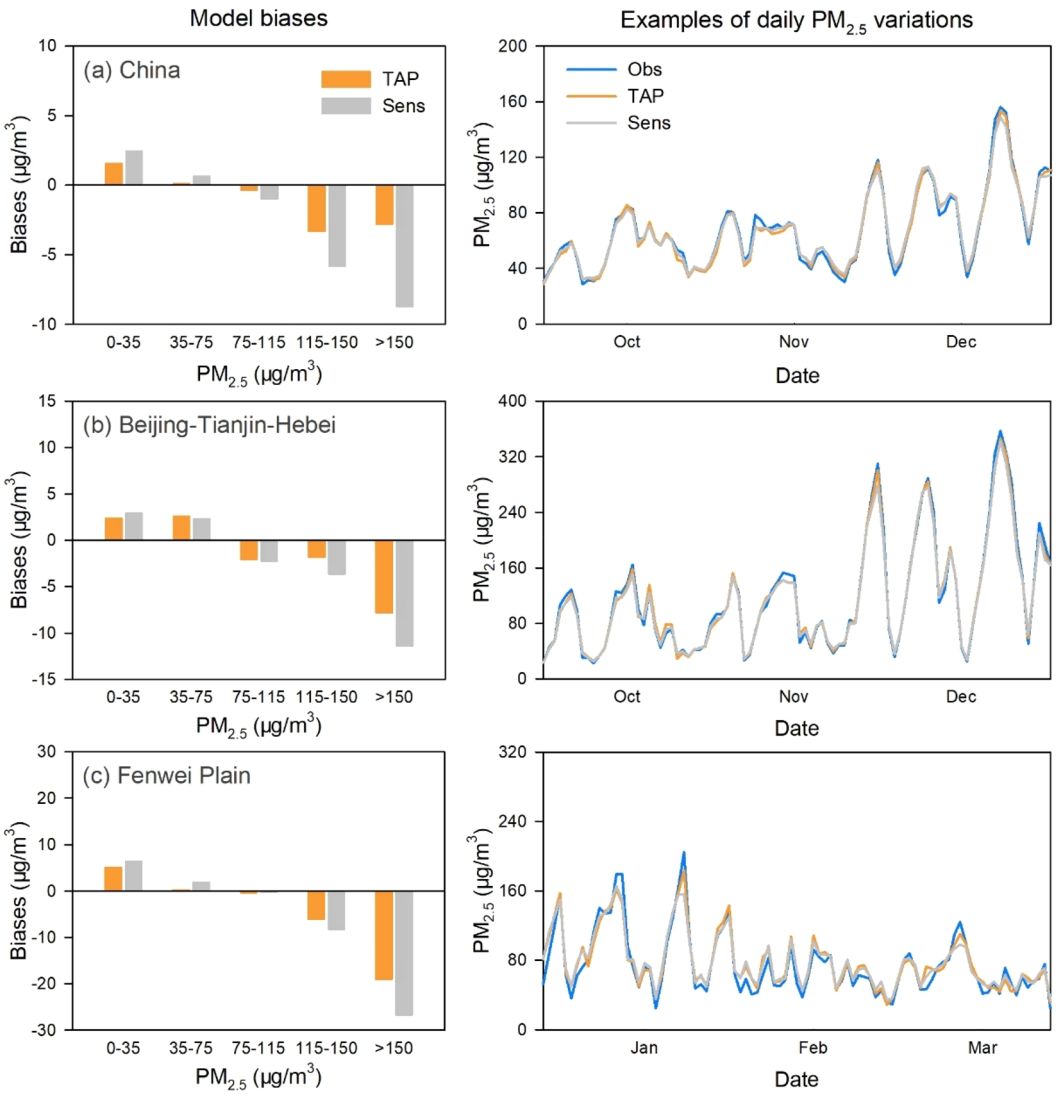


**Figure 2.** Comparison between the two-stage model in TAP and the sensitivity test model "Sens". Left column: $PM_{2.5}$ biases from TAP (orange) and Sens (gray) under different $PM_{2.5}$ pollution levels in (a) China, (b) the Beijing-Tianjin-Hebei region and (c) the Fenwei Plain. Right column: examples of daily $PM_{2.5}$ variations from ground observations (blue), TAP (orange), and Sens (gray).

For the near real-time product since Jan 2021, the training data set contains one-year data from the year 2020 and is updated every day on a rolling basis to include the most recent input data. The input data size (i.e., one year) is selected based on a series of sensitivity tests that use data of one, two, three and eight years to train the two-stage model (SI Table S1). When the size of the training data increases from one year to eight years, the time consumed to fit the model increases exponentially from hours to days (SI Table S1) while the model performance decreases slightly (SI Figure S1). Therefore, one-year data are selected in our near real-time model for both a reasonable fitting time and a good model performance. The two-stage random forest model is trained by the one-year rolling updated data set every day, and then near real-time $PM_{2.5}$ data are generated and uploaded to our website. Usually, the daily $PM_{2.5}$ prediction is generated no later than 8:25 AM Beijing time and uploaded to our website by 8:45 AM Beijing time.

## 3. EVALUATION OF MODEL PERFORMANCE

The performance of our two-stage model is evaluated through three cross-validation (CV) experiments: out-of-bag CV, spatial CV, and by-year CV. The out-of-bag CV is the most commonly used CV for the random forest models that compares the $PM_{2.5}$ measurements with the predictions of out-of-bag samples. Spatial CV evaluates the model's ability to make predictions at locations without monitors; all the monitoring stations are randomly divided into five subsets, and each time, the model is trained using data from four subsets and tested on the data from the remaining subset. Similarly, by-year CV evaluates the model's hindcast prediction ability, which sequentially selects one year of data for testing and trains the model with the data from the remaining years.

Table 2 shows the CV results of our two-stage random forest models at the daily level, including the $R^2$ and root-mean-square error (RMSE) values between the CV estimates and the ground measurements. The $PM_{2.5}$ predictions from the out-of-bag CV show good agreements compared against the ground observations, with $R^2$ of 0.80−0.88 and RMSE of 13.9−22.1 $\mu g/m^3$ for different years between 2013−2020, which indicates


https://doi.org/10.1021/acs.est.1c01863
Environ. Sci. Technol. XXXX, XXX, XXX−XXX

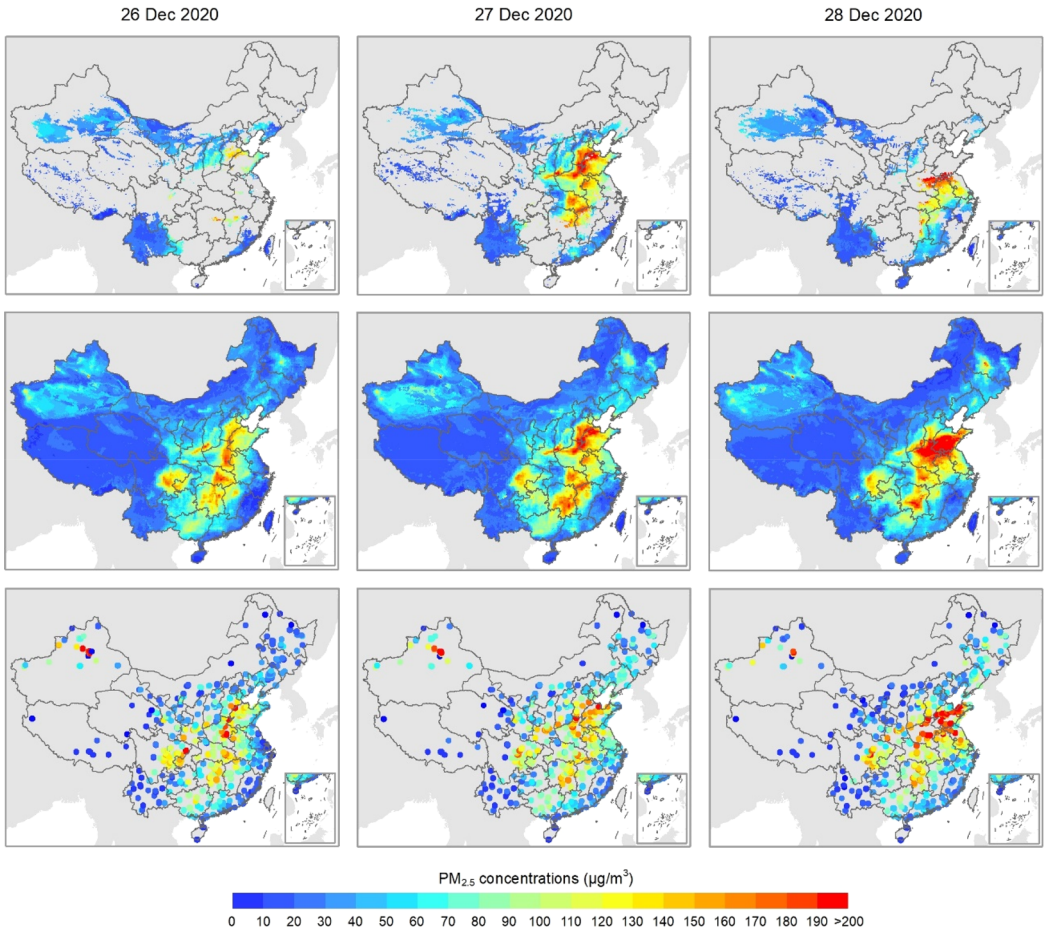


**Figure 3.** Daily full-coverage $PM_{2.5}$ concentrations from TAP (middle row) compared with estimations without gap filling (top row) and the ground observations (bottom row). Data for 26−28 December 2020 are shown as examples.

that our two-stage model is quite robust. The spatial CV $R^2$ value decreases by 0.05−0.11 when compared with the out-of-bag CV, indicating that unobserved spatial trends contribute to the $PM_{2.5}$ predictions. The model's hindcast performance further decreases in the by-year CV, with an $R^2$ of 0.58 and RMSE of 27.5 $\mu g/m^3$, reflecting a slight overfit in the hindcast of $PM_{2.5}$ in years prior to 2013.

Our model's performance is comparable to that of models presented in other studies on the basis of the $R^2$ and RMSE values shown in Table 2. The statistical or machine learning models at the 10-km grid on a daily scale have 10-fold CV $R^2$ values ranging between 0.79 and 0.80 in China,[19,22,24] which are similar to our out-of-bag CV results (i.e., 0.83 on average). Models with a 1 km grid have higher $R^2$ values,[23,28] which might be partially explained by the correlations between $PM_{2.5}$ and the 1 km AOD being higher than those between $PM_{2.5}$ and the 10 km AOD, as well as the substantial increase in collocated AOD−$PM_{2.5}$ pairs at a 1 km resolution than at a 10 km resolution for a larger sample size.[48]

## 4. ILLUSTRATION OF TAP CAPABILITIES

**4.1. Near Real-Time Updates.** Our TAP $PM_{2.5}$ product is the first near real-time $PM_{2.5}$ database in China based on multisource data, including ground measurements, satellite AOD, high-resolution emission inventories (i.e., the MEIC inventory) and WRF/CMAQ simulations. Several factors support the timely update of $PM_{2.5}$ data. First, the dynamic updates of anthropogenic emissions in China by the MEIC and the high-performance computer at Tsinghua University facilitate the operational simulation of the WRF/CMAQ model, which is an important data source for $PM_{2.5}$ estimations, as has been evaluated in previous studies.[25,28] Second, we choose the tree-based algorithm to fill the gaps in $PM_{2.5}$ concentrations, which is accurate and has reasonable speed. Other methods for filling in AOD gaps such as the multiple imputation method make use of more $PM_{2.5}$ observations in the training data set;[18] however, such a method has a much lower computation speed, and we found similar performances between these two gap-filling methods in our previous work.[30] Finally, the cloud-computing platform makes it possible to develop the model online and allows users to conveniently access all the data products. The daily data set of $PM_{2.5}$ from TAP can be found through our website in near real time.

**4.2. Improved Performance on Polluted Days.** Our two-stage model coupled with the SMOTE technique improves the $PM_{2.5}$ estimations on highly polluted days. Compared to the sensitivity test model (Sens) without SMOTE and using $PM_{2.5}$ measurements directly as the dependent variable, the two-stage model has a similar $R^2$ but higher regression slope (0.97 vs 0.94) when evaluated against ground measurements. Figure 2 shows a detailed comparison between our two-stage model and the Sens model using year 2015 as an example. Usually, $PM_{2.5}$ concentrations are underestimated over polluted days but a little overestimated


https://doi.org/10.1021/acs.est.1c01863
Environ. Sci. Technol. XXXX, XXX, XXX−XXX

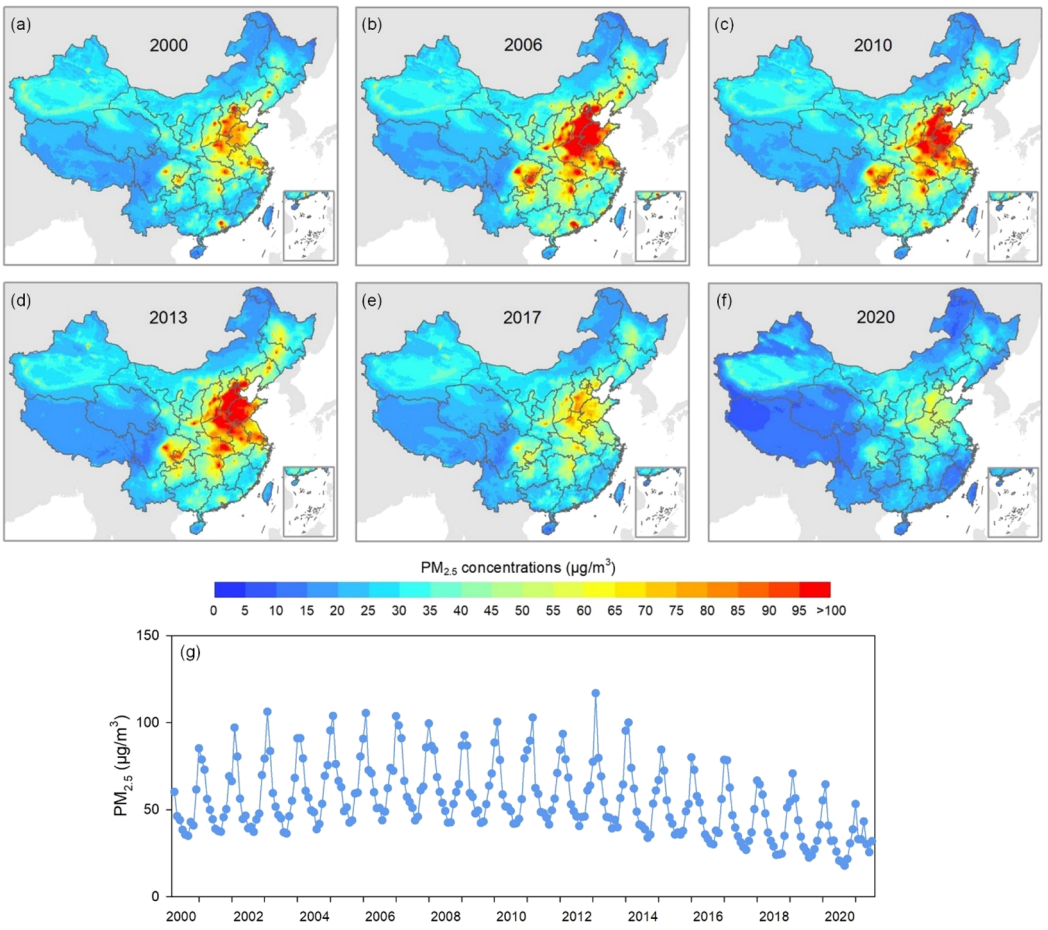


**Figure 4.** Historical data set of $PM_{2.5}$ from 2000 to the present. (a–f) Annual mean $PM_{2.5}$ concentrations for 2000, 2006, 2010, 2013, 2017, and 2020. (g) Population-weighted mean $PM_{2.5}$ in China from 2000 to the present on a monthly scale.

in clean days. After adopting our two-stage model, the mean biases over China at high $PM_{2.5}$ levels above 150 $\mu g/m^3$ decrease by 5.9 $\mu g/m^3$ (Figure 2a), and the number is even larger for the Fenwei Plain (i.e., 7.7 $\mu g/m^3$). We also present examples of the estimated daily variations in $PM_{2.5}$ concentrations from TAP and Sens and find that TAP has better ability in capturing the concentrations peaks on polluted days.

**4.3. Full-Coverage on Daily Scale.** Figure 3 shows full-coverage daily maps of the TAP $PM_{2.5}$ as well as the estimations without gap-filling and ground observations during an example period, 26–28 December 2020. On these days, satellite AOD data only cover 16%–24% of the grid cells in China; thus, many $PM_{2.5}$ concentration hotspots are missing. Such missingness might cause biases in the averaged concentrations as the missing are sometimes nonrandom. In summer, AOD data are usually missing over southern China due to rain and clouds, while in winter, AOD data over northern China are usually missing due to snow cover and haze.[49] The nonrandom distribution of missing AOD causes negative biases in the average $PM_{2.5}$ in the north and positive biases in the average $PM_{2.5}$ in the south.[18,26] After gap-filling with supportive information from the WRF/CMAQ simulations and meteorological data, the daily maps of $PM_{2.5}$ become complete and can more accurately capture the day-to-day variations in $PM_{2.5}$. For example, the TAP $PM_{2.5}$ maps successfully capture the $PM_{2.5}$ changes across the North China Plain during the haze event that occurred on 26–28 December 2020 (Figure 3). $PM_{2.5}$ pollution started to rise on 26 December 2020, and high $PM_{2.5}$ levels were found in southern Hebei and northern Shandong. Then, the pollution expanded, and on 28 December 2020, Shandong, Henan and northern Anhui were covered by haze exceeding 180 $\mu g/m^3$. Such patterns could not be captured using the $PM_{2.5}$ data without gap filling.

**4.4. Historical $PM_{2.5}$ Trends Since 2000.** The TAP $PM_{2.5}$ database is also able to provide historical trends of $PM_{2.5}$ from 2000 to the present (Figure 4). Indeed, $PM_{2.5}$ estimates prior to 2013 have larger uncertainties, as there are no observation data to calibrate and evaluate our models. The by-year CV indicates that the model's hindcast ability has a smaller $R^2$ and larger RMSE than the out-of-bag CV. However, we use the year-by-year emission inventory from MEIC and the long-term CMAQ simulations as important input data to support the $PM_{2.5}$ estimates before 2013, thereby providing the best available knowledge of the spatial and temporal trends of $PM_{2.5}$ concentrations in history over China. Moreover, the long-term satellite AOD data set also provides valuable observational evidence of aerosol changes since 2000. We believe that the long-term trend of $PM_{2.5}$ constrained by these two data sets is reliable.

We also compare the $PM_{2.5}$ trends estimated by our data with the long-term $PM_{2.5}$ data set generated by Hammer et al.[50] (2000–2018) and the CHAP data developed by Wei et al.[23] (2000–2020) (SI Figure S2). Similar trends are found for the time when ground measurements are available, except for


https://doi.org/10.1021/acs.est.1c01863
Environ. Sci. Technol. XXXX, XXX, XXX–XXX

CHAP in the pearl river delta. A possible reason is that CHAP is not gap-filled and the nonrandom missingness in AOD lead to biases in the annual mean $PM_{2.5}$ value. For the time without available ground observations, the data by Hammer et al.[50] are always lower compared to TAP and CHAP. Emission estimates over China show that primary $PM_{2.5}$ emissions and $SO_2$ emissions peaked around 2006,[34] which is more consistent with the trends estimated by TAP and CHAP.

Figure 4 shows the $PM_{2.5}$ trends since 2000 in China. The TAP data capture the $PM_{2.5}$ increase before 2006 (when there is no efficient emission control policy) and the sharp drop in $PM_{2.5}$ concentrations after 2013 (when strict control measures were implemented). The peak of the national population-weighted mean $PM_{2.5}$ concentrations occurred in 2006 (68.0 $\mu g/m^3$), the starting year of the 11th Five Year Plan (FYP, 2006−2010), when flue-gas desulfurization devices were installed in coal-fired power plants. After that, the increasing trend of $PM_{2.5}$ concentrations was reversed. Since 2013, strict clean air policies have been implemented, that is, the Air Pollution Prevention and Control Action Plan (2013−2017) and the Blue Sky Protection Campaign (2018−2020). The Air Pollution Prevention and Control Action Plan reduced the annual population-weighted mean $PM_{2.5}$ from 62.5 $\mu g/m^3$ in 2013 to 44.4 $\mu g/m^3$ in 2017, and the Blue Sky Protection Campaign further reduced the $PM_{2.5}$ concentrations to 33.1 $\mu g/m^3$ in 2020.

## 5. DISCUSSION

In this study, we develop the TAP $PM_{2.5}$ database that couples real-time ground observations, near real-time satellite data and meteorological reanalysis data, and operational simulations from the WRF/CMAQ modeling system to provide $PM_{2.5}$ concentration data that are updated in a timely manner. Based on a two-stage machine learning model and gap-filling method, TAP provides daily full-coverage $PM_{2.5}$ concentrations at a spatial resolution of 10 km in near real time. All the data are publicly available for sharing with the community.

Our work is subject to some limitations. First, our near real-time $PM_{2.5}$ products rely on the near real-time updates of all the input data (except for the land use, population and elevation data, which have update frequencies of yearly or longer). Delays in any of these data sets would influence the updates of our $PM_{2.5}$ data. Second, although we believe that the long-term spatial and temporal patterns of $PM_{2.5}$ concentrations prior to 2013 are reliable due to the reasonableness of the input data, the uncertainties in $PM_{2.5}$ on a daily scale are still larger than the daily $PM_{2.5}$ estimates after 2013. Third, the TAP $PM_{2.5}$ concentrations over the northwestern region dominated by the dust component tend to be underestimated, because MODIS AOD over bright surface (e.g., desert) are reported to have larger uncertainties compared to ground measurements[51,52] and the CMAQ $PM_{2.5}$ simulations underestimated dust concentrations severely.[10] Finally, previous studies have shown that using 1 km AOD estimates from the Multi-Angle Implementation of Atmospheric Correction (MAIAC) algorithm would improve the model performance, as a finer resolution would result in better correspondence between the AOD and $PM_{2.5}$.[48] However, building near real-time models at 1 km would cause exponential increases in the required computing resources and storage. Therefore, we choose the 10 km $PM_{2.5}$ data as our first step for the TAP database.

In the future, we will continue to improve our methods and provide more air pollutant species and finer spatial resolution data. Accordingly, we will build the TAP database into a near real-time database of multiple air pollutants at different spatial and temporal resolutions based on multiple data sources.

## ■ ASSOCIATED CONTENT

### Supporting Information

The Supporting Information is available free of charge at https://pubs.acs.org/doi/10.1021/acs.est.1c01863.

Results of the sensitivity tests that aim at examining the impact of training data size on the model performance, comparisons of the estimated long-term $PM_{2.5}$ trends during 2000−2020 between TAP and other data sets (PDF)

## ■ AUTHOR INFORMATION


### Corresponding Author

**Qiang Zhang** − *Ministry of Education Key Laboratory for Earth System Modelling, Department of Earth System Science, Tsinghua University, Beijing 100084, China*; Email: qiangzhang@tsinghua.edu.cn

### Authors

**Guannan Geng** − *State Key Joint Laboratory of Environment Simulation and Pollution Control, School of Environment, Tsinghua University, Beijing 100084, China; State Environmental Protection Key Laboratory of Sources and Control of Air Pollution Complex, Beijing 100084, China*; orcid.org/0000-0002-1605-8448

**Qingyang Xiao** − *State Key Joint Laboratory of Environment Simulation and Pollution Control, School of Environment, Tsinghua University, Beijing 100084, China*

**Shigan Liu** − *Ministry of Education Key Laboratory for Earth System Modelling, Department of Earth System Science, Tsinghua University, Beijing 100084, China*

**Xiaodong Liu** − *State Key Joint Laboratory of Environment Simulation and Pollution Control, School of Environment, Tsinghua University, Beijing 100084, China*

**Jing Cheng** − *Ministry of Education Key Laboratory for Earth System Modelling, Department of Earth System Science, Tsinghua University, Beijing 100084, China*

**Yixuan Zheng** − *Center of Air Quality Simulation and System Analysis, Chinese Academy of Environmental Planning, Beijing 100012, China*; orcid.org/0000-0002-3429-5754

**Tao Xue** − *Institute of Reproductive and Child Health, Ministry of Health Key Laboratory of Reproductive Health and Department of Epidemiology and Biostatistics, School of Public Health, Peking University, Beijing 100191, China*; orcid.org/0000-0002-7045-2307

**Dan Tong** − *Ministry of Education Key Laboratory for Earth System Modelling, Department of Earth System Science, Tsinghua University, Beijing 100084, China*; orcid.org/0000-0003-3787-0707

**Bo Zheng** − *Institute of Environment and Ecology, Tsinghua Shenzhen International Graduate School, Tsinghua University, Shenzhen 518055, China*

**Yiran Peng** − *Ministry of Education Key Laboratory for Earth System Modelling, Department of Earth System Science, Tsinghua University, Beijing 100084, China*




https://doi.org/10.1021/acs.est.1c01863
Environ. Sci. Technol. XXXX, XXX, XXX−XXX

**Xiaomeng Huang** − *Ministry of Education Key Laboratory for Earth System Modelling, Department of Earth System Science, Tsinghua University, Beijing 100084, China*
**Kebin He** − *State Key Joint Laboratory of Environment Simulation and Pollution Control, School of Environment, Tsinghua University, Beijing 100084, China; State Environmental Protection Key Laboratory of Sources and Control of Air Pollution Complex, Beijing 100084, China*

Complete contact information is available at: https://pubs.acs.org/10.1021/acs.est.1c01863

### Notes

The authors declare no competing financial interest.

## ■ ACKNOWLEDGMENTS

This work was supported by the National Natural Science Foundation of China (42005135, 42007189, 41921005, and 41625020).

## ■ REFERENCES

(1) Forouzanfar, M. H.; Afshin, A.; Alexander, L. T.; Anderson, H. R.; Bhutta, Z. A.; Biryukov, S.; Brauer, M.; Burnett, R.; Cercy, K.; Charlson, F. J. Global, regional, and national comparative risk assessment of 79 behavioural, environmental and occupational, and metabolic risks or clusters of risks, 1990−2015: a systematic analysis for the Global Burden of Disease Study 2015. *Lancet* **2016**, *388* (10053), 1659−1724.

(2) Seinfeld, J. H.; Pandis, S. N. *Atmospheric Chemistry and Physics: From Air Pollution to Climate Change*; John Wiley & Sons, 2016.

(3) Burnett, R.; Chen, H.; Szyszkowicz, M.; Fann, N.; Hubbell, B.; Pope, C. A.; Apte, J. S.; Brauer, M.; Cohen, A.; Weichenthal, S.; Coggins, J.; Di, Q.; Brunekreef, B.; Frostad, J.; Lim, S. S.; Kan, H.; Walker, K. D.; Thurston, G. D.; Hayes, R. B.; Lim, C. C.; Turner, M. C.; Jerrett, M.; Krewski, D.; Gapstur, S. M.; Diver, W. R.; Ostro, B.; Goldberg, D.; Crouse, D. L.; Martin, R. V.; Peters, P.; Pinault, L.; Tjepkema, M.; van Donkelaar, A.; Villeneuve, P. J.; Miller, A. B.; Yin, P.; Zhou, M.; Wang, L.; Janssen, N. A. H.; Marra, M.; Atkinson, R. W.; Tsang, H.; Quoc Thach, T.; Cannon, J. B.; Allen, R. T.; Hart, J. E.; Laden, F.; Cesaroni, G.; Forastiere, F.; Weinmayr, G.; Jaensch, A.; Nagel, G.; Concin, H.; Spadaro, J. V. Global estimates of mortality associated with long-term exposure to outdoor fine particulate matter. *Proc. Natl. Acad. Sci. U. S. A.* **2018**, *115* (38), 9592−9597.

(4) Cohen, A. J.; Brauer, M.; Burnett, R.; Anderson, H. R.; Frostad, J.; Estep, K.; Balakrishnan, K.; Brunekreef, B.; Dandona, L.; Dandona, R.; Feigin, V.; Freedman, G.; Hubbell, B.; Jobling, A.; Kan, H.; Knibbs, L.; Liu, Y.; Martin, R.; Morawska, L.; Pope, C. A.; Shin, H.; Straif, K.; Shaddick, G.; Thomas, M.; van Dingenen, R.; van Donkelaar, A.; Vos, T.; Murray, C. J. L.; Forouzanfar, M. H. Estimates and 25-year trends of the global burden of disease attributable to ambient air pollution: an analysis of data from the Global Burden of Diseases Study 2015. *Lancet* **2017**, *389* (10082), 1907−1918.

(5) Che, H.; Zhang, X.; Li, Y.; Zhou, Z.; Qu, J. J., Horizontal visibility trends in China 1981−2005. *Geophys. Res. Lett.* **2007**, *34*, (24). DOI: 10.1029/2007GL031450

(6) Xiao, Q.; Chen, H.; Strickland, M. J.; Kan, H.; Chang, H. H.; Klein, M.; Yang, C.; Meng, X.; Liu, Y. Associations between birth outcomes and maternal PM2. 5 exposure in Shanghai: a comparison of three exposure assessment approaches. *Environ. Int.* **2018**, *117*, 226−236.

(7) Strickland, M. J.; Hao, H.; Hu, X.; Chang, H. H.; Darrow, L. A.; Liu, Y. Pediatric emergency visits and short-term changes in PM2. 5 concentrations in the US State of Georgia. *Environ. Health Perspect.* **2016**, *124* (5), 690−696.

(8) Geng, G.; Xiao, Q.; Zheng, Y.; Tong, D.; Zhang, Y.; Zhang, X.; Zhang, Q.; He, K.; Liu, Y. Impact of China's Air Pollution Prevention and Control Action Plan on PM2.5 chemical composition over eastern China. *Sci. China: Earth Sci.* **2019**, *62* (12), 1872−1884.

(9) Geng, G.; Zhang, Q.; Tong, D.; Li, M.; Zheng, Y.; Wang, S.; He, K. Chemical composition of ambient PM2.5 over China and relationship to precursor emissions during 2005−2012. *Atmos. Chem. Phys.* **2017**, *17* (14), 9187.

(10) Zhang, Q.; Zheng, Y.; Tong, D.; Shao, M.; Wang, S.; Zhang, Y.; Xu, X.; Wang, J.; He, H.; Liu, W.; Ding, Y.; Lei, Y.; Li, J.; Wang, Z.; Zhang, X.; Wang, Y.; Cheng, J.; Liu, Y.; Shi, Q.; Yan, L.; Geng, G.; Hong, C.; Li, M.; Liu, F.; Zheng, B.; Cao, J.; Ding, A.; Gao, J.; Fu, Q.; Huo, J.; Liu, B.; Liu, Z.; Yang, F.; He, K.; Hao, J. Drivers of improved PM2.5 air quality in China from 2013 to 2017. *Proc. Natl. Acad. Sci. U. S. A.* **2019**, *116*, 201907956.

(11) Xiao, Q.; Geng, G.; Liang, F.; Wang, X.; Lv, Z.; Lei, Y.; Huang, X.; Zhang, Q.; Liu, Y.; He, K. Changes in spatial patterns of PM2.5 pollution in China 2000−2018: Impact of clean air policies. *Environ. Int.* **2020**, *141*, 105776.

(12) Bai, K.; Li, K.; Wu, C.; Chang, N. B.; Guo, J. A homogenized daily in situ PM2.5 concentration dataset from the national air quality monitoring network in China. *Earth Syst. Sci. Data* **2020**, *12* (4), 3067−3080.

(13) Xing, J.; Mathur, R.; Pleim, J.; Hogrefe, C.; Gan, C.-M.; Wong, D.-C.; Wei, C.; Gilliam, R.; Pouliot, G. Observations and modeling of air quality trends over 1990−2010 across the Northern Hemisphere: China, the United States and Europe. *Atmos. Chem. Phys.* **2015**, *15* (5), 2723−2747.

(14) Zhang, Q.; Streets, D. G.; Carmichael, G. R.; He, K.; Huo, H.; Kannari, A.; Klimont, Z.; Park, I.; Reddy, S.; Fu, J. Asian emissions in 2006 for the NASA INTEX-B mission. *Atmos. Chem. Phys.* **2009**, *9* (14), 5131−5153.

(15) Zheng, B.; Zhang, Q.; Zhang, Y.; He, K. B.; Wang, K.; Zheng, G. J.; Duan, F. K.; Ma, Y. L.; Kimoto, T. Heterogeneous chemistry: a mechanism missing in current models to explain secondary inorganic aerosol formation during the January 2013 haze episode in North China. *Atmos. Chem. Phys.* **2015**, *15* (4), 2031−2049.

(16) Wang, Y.; Zhang, Q.; Jiang, J.; Zhou, W.; Wang, B.; He, K.; Duan, F.; Zhang, Q.; Philip, S.; Xie, Y. Enhanced sulfate formation during China's severe winter haze episode in January 2013 missing from current models. *Journal of Geophysical Research: Atmospheres* **2014**, *119* (17), 10,425−10,440.

(17) Baek, J.; Hu, Y.; Odman, M. T.; Russell, A. G. Modeling secondary organic aerosol in CMAQ using multigenerational oxidation of semi-volatile organic compounds. *Journal of Geophysical Research: Atmospheres* **2011**, *116*, D22.

(18) Xiao, Q.; Wang, Y.; Chang, H. H.; Meng, X.; Geng, G.; Lyapustin, A.; Liu, Y. Full-coverage high-resolution daily PM2.5 estimation using MAIAC AOD in the Yangtze River Delta of China. *Remote Sensing of Environment* **2017**, *199* (Supplement C), 437−446.

(19) Fang, X.; Zou, B.; Liu, X.; Sternberg, T.; Zhai, L. Satellite-based ground PM2.5 estimation using timely structure adaptive modeling. *Remote Sensing of Environment* **2016**, *186*, 152−163.

(20) Liang, F.; Xiao, Q.; Huang, K.; Yang, X.; Liu, F.; Li, J.; Lu, X.; Liu, Y.; Gu, D. The 17-y spatiotemporal trend of $PM_{2.5}$ and its mortality burden in China. *Proc. Natl. Acad. Sci. U. S. A.* **2020**, *117* (41), 25601−25608.

(21) Lin, C. Q.; Liu, G.; Lau, A. K. H.; Li, Y.; Li, C. C.; Fung, J. C. H.; Lao, X. Q. High-resolution satellite remote sensing of provincial PM2.5 trends in China from 2001 to 2015. *Atmos. Environ.* **2018**, *180*, 110−116.

(22) Ma, Z.; Hu, X.; Sayer, A. M.; Levy, R.; Zhang, Q.; Xue, Y.; Tong, S.; Bi, J.; Huang, L.; Liu, Y. Satellite-Based Spatiotemporal Trends in PM2.5 Concentrations: China, 2004−2013. *Environ. Health Perspect.* **2016**, *124* (2), 184−192.

(23) Wei, J.; Li, Z.; Lyapustin, A.; Sun, L.; Peng, Y.; Xue, W.; Su, T.; Cribb, M. Reconstructing 1-km-resolution high-quality PM2.5 data records from 2000 to 2018 in China: spatiotemporal variations and policy implications. *Remote Sensing of Environment* **2021**, *252*, 112136.

(24) Xiao, Q.; Chang, H. H.; Geng, G.; Liu, Y. An ensemble machine-learning model to predict historical PM2.5 concentrations in

China from satellite data. *Environ. Sci. Technol.* **2018**, *52* (22), 13260−13269.
(25) Xue, T.; Zheng, Y.; Tong, D.; Zheng, B.; Li, X.; Zhu, T.; Zhang, Q. Spatiotemporal continuous estimates of PM2.5 concentrations in China, 2000−2016: A machine learning method with inputs from satellites, chemical transport model, and ground observations. *Environ. Int.* **2019**, *123*, 345−357.
(26) Geng, G.; Zhang, Q.; Martin, R. V.; van Donkelaar, A.; Huo, H.; Che, H.; Lin, J.; He, K. Estimating long-term PM2.5 concentrations in China using satellite-based aerosol optical depth and a chemical transport model. *Remote Sensing of Environment* **2015**, *166*, 262−270.
(27) Kong, L.; Tang, X.; Zhu, J.; Wang, Z.; Li, J.; Wu, H.; Wu, Q.; Chen, H.; Zhu, L.; Wang, W.; Liu, B.; Wang, Q.; Chen, D.; Pan, Y.; Song, T.; Li, F.; Zheng, H.; Jia, G.; Lu, M.; Wu, L.; Carmichael, G. R. A Six-year long (2013−2018) High-resolution Air Quality Reanalysis Dataset over China base on the assimilation of surface observations from CNEMC. *Earth Syst. Sci. Data Discuss.* **2020**, *2020*, 1−44.
(28) Huang, C.; Hu, J.; Xue, T.; Xu, H.; Wang, M., High-Resolution Spatiotemporal Modeling for Ambient PM2.5 Exposure Assessment in China from 2013 to 2019. *Environ. Sci. Technol.* **2021**.*55*2152
(29) Wei, J.; Li, Z.; Cribb, M.; Huang, W.; Xue, W.; Sun, L.; Guo, J.; Peng, Y.; Li, J.; Lyapustin, A.; Liu, L.; Wu, H.; Song, Y. Improved 1-km resolution PM2.5 estimates across China using enhanced space-time extremely randomized trees. *Atmos. Chem. Phys.* **2020**, *20* (6), 3273−3289.
(30) Xiao, Q.; Geng, G.; Cheng, J.; Liang, F.; Li, R.; Meng, X.; Xue, T.; Huang, X.; Kan, H.; Zhang, Q.; He, K. Evaluation of gap-filling approaches in satellite-based daily PM2.5 prediction models. *Atmos. Environ.* **2021**, *244*, 117921.
(31) Levy, R.; Mattoo, S.; Munchak, L.; Remer, L.; Sayer, A.; Patadia, F.; Hsu, N. The Collection 6 MODIS aerosol products over land and ocean. *Atmos. Meas. Tech.* **2013**, *6* (11), 2989.
(32) Hsu, N.; Jeong, M. J.; Bettenhausen, C.; Sayer, A.; Hansell, R.; Seftor, C.; Huang, J.; Tsay, S. C. Enhanced Deep Blue aerosol retrieval algorithm: The second generation. *Journal of Geophysical Research: Atmospheres* **2013**, *118* (16), 9296−9315.
(33) Jinnagara Puttaswamy, S.; Nguyen, H. M.; Braverman, A.; Hu, X.; Liu, Y. Statistical data fusion of multi-sensor AOD over the continental United States. *Geocarto International* **2014**, *29* (1), 48−64.
(34) Li, M.; Liu, H.; Geng, G.; Hong, C.; Liu, F.; Song, Y.; Tong, D.; Zheng, B.; Cui, H.; Man, H. Anthropogenic emission inventories in China: a review. *National Science Review* **2017**, *4* (6), 834−866.
(35) Zheng, B.; Tong, D.; Li, M.; Liu, F.; Hong, C.; Geng, G.; Li, H.; Li, X.; Peng, L.; Qi, J.; Yan, L.; Zhang, Y.; Zhao, H.; Zheng, Y.; He, K.; Zhang, Q. Trends in China's anthropogenic emissions since 2010 as the consequence of clean air actions. *Atmos. Chem. Phys.* **2018**, *18* (19), 14095−14111.
(36) Zheng, B.; Zhang, Q.; Geng, G.; Shi, Q.; Lei, Y.; He, K. Changes in China's anthropogenic emissions during the COVID-19 pandemic. *Earth Syst. Sci. Data Discuss.* **2021**, *2020*, 1−20.
(37) Gelaro, R.; McCarty, W.; Suárez, M. J.; Todling, R.; Molod, A.; Takacs, L.; Randles, C. A.; Darmenov, A.; Bosilovich, M. G.; Reichle, R.; Wargan, K.; Coy, L.; Cullather, R.; Draper, C.; Akella, S.; Buchard, V.; Conaty, A.; da Silva, A. M.; Gu, W.; Kim, G.-K.; Koster, R.; Lucchesi, R.; Merkova, D.; Nielsen, J. E.; Partyka, G.; Pawson, S.; Putman, W.; Rienecker, M.; Schubert, S. D.; Sienkiewicz, M.; Zhao, B. The Modern-Era Retrospective Analysis for Research and Applications, Version 2 (MERRA-2). *J. Clim.* **2017**, *30* (14), 5419−5454.
(38) Lucchesi, R. File Specification for GEOS-5 FP (*Forward Processing*). **2013**.
(39) Gong, P.; Li, X.; Zhang, W. 40-Year (1978−2017) human settlement changes in China reflected by impervious surfaces from satellite remote sensing. *Science Bulletin* **2019**, *64* (11), 756−763.
(40) Cheng, J.; Su, J.; Cui, T.; Li, X.; Dong, X.; Sun, F.; Yang, Y.; Tong, D.; Zheng, Y.; Li, Y.; Li, J.; Zhang, Q.; He, K. Dominant role of emission reduction in PM2.5 air quality improvement in Beijing during 2013−2017: a model-based decomposition analysis. *Atmos. Chem. Phys.* **2019**, *19* (9), 6125−6146.
(41) Kain, J. S. The Kain?Fritsch Convective Parameterization: An Update. *Journal of Applied Meteorology* **2004**, *43* (1), 170−181.
(42) Grell, G. A.; Freitas, S. R. A scale and aerosol aware stochastic convective parameterization for weather and air quality modeling. *Atmos. Chem. Phys.* **2014**, *14* (10), 5233−5250.
(43) Li, M.; Zhang, Q.; Kurokawa, J.-i.; Woo, J.-H.; He, K.; Lu, Z.; Ohara, T.; Song, Y.; Streets, D. G.; Carmichael, G. R., MIX: a mosaic Asian anthropogenic emission inventory under the international collaboration framework of the MICS-Asia and HTAP. *Atmos. Chem. Phys.* **2017**, *17*, (2).935
(44) Guenther, A. B.; Jiang, X.; Heald, C. L.; Sakulyanontvittaya, T.; Duhl, T.; Emmons, L. K.; Wang, X. The Model of Emissions of Gases and Aerosols from Nature version 2.1 (MEGAN2.1): an extended and updated framework for modeling biogenic emissions. *Geosci. Model Dev.* **2012**, *5* (6), 1471−1492.
(45) Zheng, Y.; Xue, T.; Zhang, Q.; Geng, G.; Tong, D.; Li, X.; He, K. Air quality improvements and health benefits from China's clean air action since 2013. *Environ. Res. Lett.* **2017**, *12* (11), 114020.
(46) Xiao, Q.; Zheng, Y.; Geng, G.; Chen, C.; Huang, X.; Che, H.; Zhang, X.; He, K.; Zhang, Q. Separating emission and meteorological contribution to PM2.5 trends over East China during 2000−2018. *Atmos. Chem. Phys.* **2021**, *2021*, 1−32.
(47) Brokamp, C.; Jandarov, R.; Hossain, M.; Ryan, P. Predicting Daily Urban Fine Particulate Matter Concentrations Using a Random Forest Model. *Environ. Sci. Technol.* **2018**, *52* (7), 4173−4179.
(48) Chudnovsky, A.; Tang, C.; Lyapustin, A.; Wang, Y.; Schwartz, J.; Koutrakis, P. A critical assessment of high-resolution aerosol optical depth retrievals for fine particulate matter predictions. *Atmos. Chem. Phys.* **2013**, *13* (21), 10907−10917.
(49) Van Donkelaar, A.; Martin, R. V.; Levy, R. C.; da Silva, A. M.; Krzyzanowski, M.; Chubarova, N. E.; Semutnikova, E.; Cohen, A. J. Satellite-based estimates of ground-level fine particulate matter during extreme events: A case study of the Moscow fires in 2010. *Atmos. Environ.* **2011**, *45* (34), 6225−6232.
(50) Hammer, M. S.; van Donkelaar, A.; Li, C.; Lyapustin, A.; Sayer, A. M.; Hsu, N. C.; Levy, R. C.; Garay, M. J.; Kalashnikova, O. V.; Kahn, R. A.; Brauer, M.; Apte, J. S.; Henze, D. K.; Zhang, L.; Zhang, Q.; Ford, B.; Pierce, J. R.; Martin, R. V. Global Estimates and Long-Term Trends of Fine Particulate Matter Concentrations (1998−2018). *Environ. Sci. Technol.* **2020**, *54* (13), 7879−7890.
(51) Tao, M.; Chen, L.; Wang, Z.; Wang, J.; Che, H.; Xu, X.; Wang, W.; Tao, J.; Zhu, H.; Hou, C. Evaluation of MODIS Deep Blue Aerosol Algorithm in Desert Region of East Asia: Ground Validation and Intercomparison. *Journal of Geophysical Research: Atmospheres* **2017**, *122* (19), 10,357−10,368.
(52) Tao, M.; Chen, L.; Wang, Z.; Tao, J.; Che, H.; Wang, X.; Wang, Y. Comparison and evaluation of the MODIS Collection 6 aerosol data in China. *Journal of Geophysical Research: Atmospheres* **2015**, *120* (14), 6992−7005.
(53) He, Q.; Huang, B. Satellite-based mapping of daily high-resolution ground PM2.5 in China via space-time regression modeling. *Remote Sensing of Environment* **2018**, *206*, 72−83.


https://doi.org/10.1021/acs.est.1c01863
*Environ. Sci. Technol.* XXXX, XXX, XXX−XXX